

Mitigating clogging of nESI with nonvolatile buffers that mimic biological samples by induced alternative voltage

REN Mengting, HUANG Guangming*

Department of Chemistry, School of Chemistry and Materials Science, University of Science and Technology of China, Hefei 230026, China

*Corresponding author: gmhuang@ustc.edu.cn

Abstract: The detection of biological samples requires the adaptation of nanoelectrospray ionization mass spectrometry (nESI-MS) to harsher conditions, such as high concentrations nonvolatile buffers and sub-micrometer scale capillary tips. The two above-mentioned requirements would pose a considerable challenge, clogging, to nESI-MS. Herein, to mitigate the clogging problem, an induced alternative voltage was applied on the nanoemitters, which had inner diameter of less than 1 μm , with the infusion of a high-concentration salt solution, to induce electrospray ionization. The tips lifetime of the modified nESI was found to be 1~2 orders of magnitude longer than that of conventional nESI. The much longer spray time could be attributed to the re-dissolution effect of salt crystals owing to the periodic change in the electric field direction. Meanwhile, the signal of the modified nESI remained stable and sensitive even after a long run (~ 10 min) for analysis of high-concentration salt solutions. Finally, the mimic extracellular fluid and intracellular fluid were both evaluated, and the result indicated that the application of an induced alternating current voltage can be a widely applicable method to delay clogging during biological sample analysis.

Keywords: induced nESI; biological sample; clogging; submicro-capillary; spray time

CLC number: O657.63 **Document code:** A

1 Introduction

Nanoelectrospray ionization mass spectrometry (nESI-MS)^[1,2] now is an indispensable tool for analyzing both small molecules and biomacromolecules. That is because the small capillary tip can generate small-sized initial droplets that improve the sensitivity and detection limit. In these years, nESI based on capillary tips with sub-micrometer-scale has been reported by Williams et al.^[3,4] and Xu et al.^[5]. They directly used the tips with an inner diameter (i.d.) of several hundred nanometers to analyze high-concentration salt solutions in nESI. Compared to micro-sized tips, the much smaller emitter size led to a significant improvement in the signal-to-noise ratio (SNR) of the analyte ions via the reduction of salt adductions.

However, the use of smaller emitters would aggravate the clogging problem^[1,6-8]. This is relatively severe for spraying biological solutions with nonvolatile inorganic salts, which leads to the precipitation of salt crystals, thereby ensuing capillary tip clogging such that spray time are extremely shortened and resulting in unstable and unpredictable MS signals, which

considerably affects qualitative and quantitative analysis.

A few efforts have been undertaken toward preventing the capillary clogging problem. For instance, the porous polymer monolith capillary^[9-11] has enhanced resistance to clogging because the multiple flow paths continue to allow liquid flow through to the capillary tip. Nevertheless, the biological samples were not considered in these studies. In addition, keeping the tip diameter of the capillary large enough, like disposable pipette tips^[12] or chemical etching^[13], to prevent the tip from clogging seems to be a viable option, however, the sensitivity would be sacrificed. Therefore, maintaining a balance between the advantages of increased sensitivity and steadily extending spray duration during nESI for directly analyzing bio-sample solutions remains difficult.

In recent years, it has been reported that induced nESI^[14-16] has the capability to deal with chemical molecular identifications for raw biological samples, which generally pose clogging issues during conventional nESI. In this study, we aim to use a similar strategy for nESI with much smaller emitters and nonvolatile buffers to mitigate the clogging problem. Here, an alternative current voltage is applied on the

outside of nanoemitters with the infusion of high-concentration salt solutions to induce electrospray ionization. The tips lifetime of induced nESI could be 1 ~ 2 orders of magnitude longer than that of conventional nESI. Thereafter, we explored the possible reasons for mitigating clogging and investigated the sensitivity and stability of MS signals during the long-time electrospray processes under various conditions. Finally, we compared the lifetime difference between the two voltage modes based on the mimic extracellular and intracellular fluids without any pretreatment.

2 Experimental section

NaCl, KCl, CaCl₂, MgCl₂, NaHCO₃, Na₂HPO₄ and NaH₂PO₄ were purchased from Sinopharm Chemical Reagent (Shanghai) Co., Ltd. Angiotensin acetate, glucose and HEPES were purchased from Sango Biotech (Shanghai) Co., Ltd. Atenolol was purchased from Sigma-Aldrich (St Louis, MO, USA). Deionized water (18.2 M Ω · cm) was prepared using a Milli-Q system. All the reagents were used without further purification. Borosilicate glass capillaries (i. d. = 0.5 mm; outer diameter, o. d. = 1 mm) were purchased from Sutter Instruments. The capillary tip sizes before (Fig. 1(b)①) and after 5 min of the electrospray process (Fig. 1(b)②)

were prepared using a laser puller (P-2000, Sutter Instrument) and characterized via Schottky field emission scanning electron microscope (SIRION 200) and field emission scanning electron microscope (Gemini SEM 500). There were some inconsistencies between the capillary tips before and after the electrospray process (such as the inside diameter and morphology), because the two images were not of the same capillary since one capillary had to be broken off to retain an ~ 5 mm tip length for SEM analysis to (which was unusable for MS analysis). The tip features during nESI process were filmed using a camera under a biological microscope (SMART). The conventional nESI was initiated by applying a direct current voltage of approximately 1.5 ~ 2.0 kV on a silver wire (o. d. = 0.2 mm) that was inserted into the capillary and in contact with the sample solution (Fig. 1(a), top). For induced nESI, an alternating current voltage with an amplitude of 2.0 ~ 3.0 kV at 500 Hz was applied at copper sheet outside of the capillary (Fig. 1(a), down). The tips of the capillaries were all placed ~ 5 mm away from the orifice of the MS instrument. The magnitude of the voltage and the distance from the tip to the inlet in the experiments were chosen based on the good feasibility of the experiment and to avoid interference from other factors

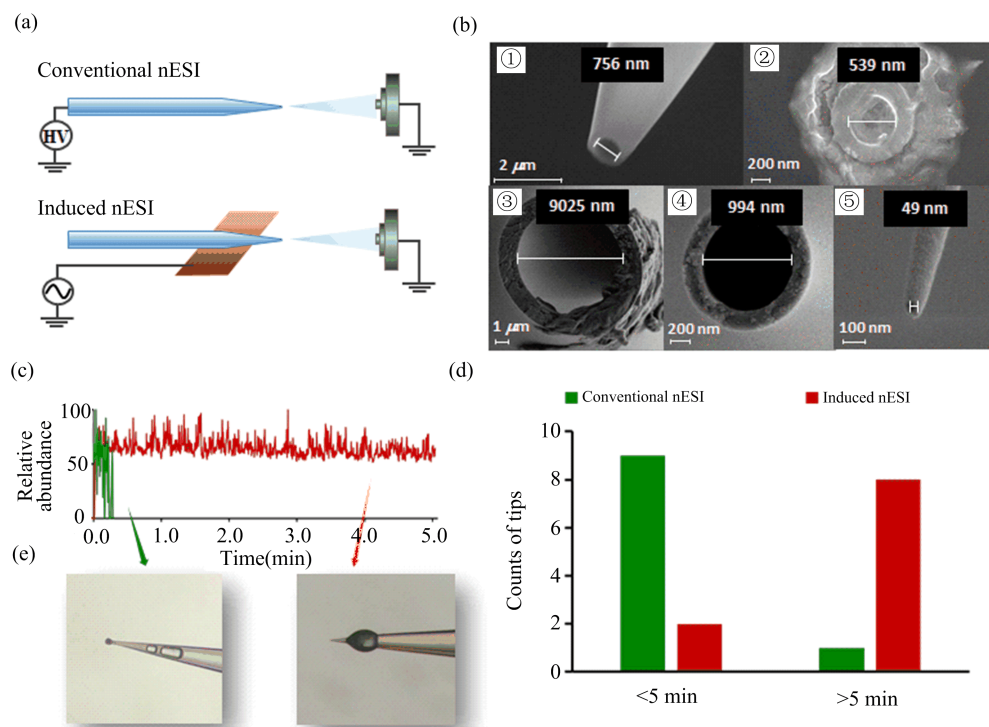


Fig. 1 (a) Schematic diagram of different voltages applied on the nanoemitters: conventional nESI applied by direct current (top) and induced nESI applied by alternative current (non-electrode contact) (down). (b) Scanning electron micrograph of emitter pulled with a series of tip i. d. less than 1 μ m. (c) Total ion current (TIC) of induced nESI (red) and conventional nESI (green) for direct infusion of the salt solution (containing 200 mmol · L⁻¹ NaCl, 1.2 mol · L⁻¹ NaH₂PO₄, 10 mmol · L⁻¹ glucose). (d) Tips counts spread over two spray time ranges in conventional nESI (n = 10) and induced nESI (n = 10). (e) Photographs of the nanoemitters sprayed by conventional nESI (left) and induced nESI (right, discontinued by operator).

such as the burning effect^[17]. Mass measurements were performed with the LTQ Velos Pro mass spectrometer (Thermo Scientific, San Jose, CA, USA). MS inlet temperature was 275 °C and the S-lens RF levels were 60% (positive mode). All data were acquired via the Xcalibur software.

3 Results and discussion

3.1 Effects of conventional nESI and induced nESI on the tip clogging

To prove that induced nESI can effectively prevent nanoemitters from clogging during submicro-nESI, we made a comparison between conventional nESI and induced nESI by using a submicro-capillary for a highly concentrated salt solution. Notably, NaCl is necessary and important in biological systems as a nonvolatile inorganic salt. Thus, we initially prepared a model salt system with 200 mmol · L⁻¹ of NaCl (in addition to 1.2 mol · L⁻¹ NaH₂PO₄ and 10 mmol · L⁻¹ glucose, in accordance to the components of cerebrospinal fluid^[16]). Fig. 1(c) shows the spray time of the two nanoemitters by using different nESI modes. It is evident that the nanoemitter in conventional nESI process can only spray for about 0.3 min. After that the ion current went through for a period of disruption or disappeared immediately. However, the electrospray lasted for more than 5 min and the signals were relatively stable in induced nESI. This experiment suggests that the spray time of nanoemitters in induced nESI is generally at least one order of magnitude longer than that in conventional nESI.

In addition, after the electrospray process, the two nanoemitters were checked visually using an optical microscope. It was observed that a cluster of NaCl crystals were accumulated at the tip of the nanoemitter after the conventional nESI process, which was the crystallization of the NaCl (Fig. 1(e), left). This crystallization phenomenon may be attributed to the nonvolatile salt solution that filled the small-sized tip, where the rate of solvent evaporation exceeded that of the solution flow^[7,18], and the interfacial precipitation^[19] could also likely occur. Conversely, after the induced nESI process, there was no NaCl cluster found on the tip of the nanoemitter, but a large droplet attached to the outer wall of the tip, which might be the sample solution that flowed from the inside of the nanoemitter (Fig. 1(e), right).

To eliminate the randomness of the experiment, we used ten nanoemitters for the two nESI modes respectively. The spray time distribution maps of the two modes are shown in Fig. 1(d). The ratio of induced nESI to conventional nESI for spray time less than 5 min was 2/9. However, the ratio for spray time exceeding 5 min was 8/1. From the above, it can be concluded that

induced nESI can effectively prevent tips from clogging and extend the lifetime of nanoemitters compared to conventional nESI.

3.2 Dynamic status of tips in conventional and induced nESI

To verify the effects of the periodic change in the electric field direction of the alternating voltage in induced nESI, the photographs of the nanoemitters sprayed using the two modes were taken. Fig. 2(a) illustrates that the tip of the nanoemitter sprayed by conventional nESI with direct current voltage, had no abnormal change in the first 10 s, but the salt crystals started to form until 26 s. The cluster of crystals failed to be ejected by high voltage but grew up with time. Accompanied by the formation of tip clogging, bubbles were produced inside the capillary that might aggravate the clogging. It should be noted that the bubbles were not formed by the gas produced by the electrochemical reactions occurring at the metal electrode^[20]. This is because the electrode was far away from the tip and no bubbles were observed moving towards the tip from the electrode, but they were generated immediately when the clogging happened (Fig. 2(a)).

While in induced nESI process, there was a liquid drop generated on the outside of the capillary at 10 s (Fig. 2(b)). Unlike its direct current voltage counterpart, the droplet was not only continuously ejected from a sharp Taylor cone, but also back-flowed on the outer wall of the tip. This might be ascribed to the induced alternating current voltage that facilitates the behavior of the micro-sized droplet. When an alternating voltage with a certain frequency (such as 500 Hz) was applied on the outside of the capillary, the electrospray process was induced. Here, the direction of the electric field switched periodically according to the frequency. In one switching period, if the electric field is oriented towards the needle tip in the former half of the cycle, despite the change in the orientation of the electric field in the latter

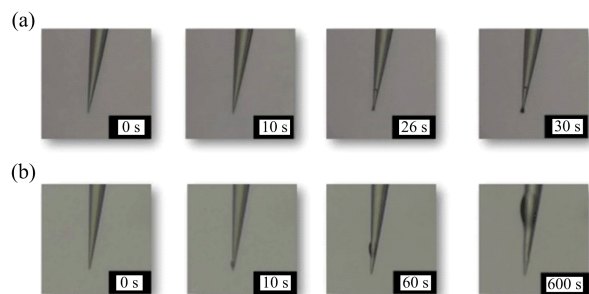


Fig. 2 Photos of nanoemitters being sprayed by (a) conventional nESI with direct current voltage which was clogged in 26 s with salt accumulation on the tip, and (b) induced nESI with alternative current voltage (non-electrode contact), which continued working in 600 s, a back-flow on the outside of the nESI emitter can be observed.

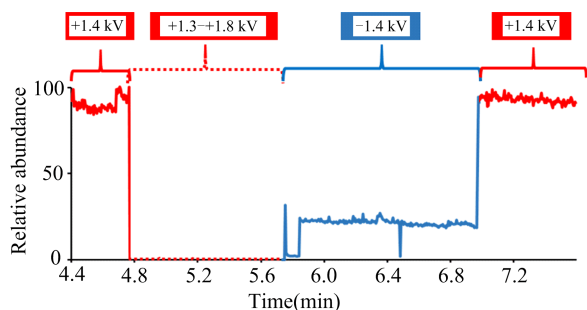


Fig. 3 TIC of conventional nESI with voltage polarity switching.

half of the cycle, the Maxwell-Wagner electric stress^[21] still remained oriented in the direction of the needle tip. Thus, the liquid drop was flattened around the tip orifice and receded up the needle as an apparent electrowetting effect. Hence, it is quite reasonable that the Maxwell stresses lead to liquid plug creeping along the outer wall of the capillary, where the salt crystals at the tip dissolved. This may explain why no crystallization was observed in induced nESI process.

As indicated by the preliminary experimental results, we assumed that the reason for the retarded tip clogging with the induced alternating voltage would be related to the periodic change in the electric field stress^[1,22,23]. To further verify this possibility, the capillary (tip with i.d. = 3 μm) was electrosprayed, using a 300 $\text{mmol} \cdot \text{L}^{-1}$ NaCl aqueous solution as the model, followed by the application of a direct current voltage. As shown in Fig. 3, a stable and abundant ion current

remained until approximately 4.8 min in positive mode (left, red solid line), which disappeared even when the direct current voltage was adjusted from +1.3 to +1.8 kV. However, the crystals still failed to jet out (red dashed line). While spraying in negative mode for approximately 1 min (blue solid line), the signal picked up again (right, red solid line), thereby indicating the tip of the nanoemitter could be reopened by an oppositely directed force^[21] that may be a combination of mechanical and electrical stresses^[1] owing to the variation in the potential.

3.3 Investigation of the performance of induced nESI under various conditions

For induced nESI, the signals of the analyte were almost similar during several minutes of analysis. Fig. 4 illustrates the intensity of atenolol [$\text{C}_{14}\text{H}_{22}\text{N}_2\text{O}_3 + \text{H}^+$] changed only by 2.4% from 0.5 to 9.5 min. This result indicates that there was no significant change in sensitivity along with time in induced nESI. Furthermore, it has been proposed that the desalting effect is related to the size of spray tips, possibly because less nonvolatile salts coexist with large biomolecules in small droplets (small tip size)^[3,4], and the effect can be attributed to proton-enrichment with smaller droplets^[5]. Fig. 5 illustrates that the SNR of angiotensin II in Tris buffer solution increased from 6.1 to 41.6 with the reduction of tip diameters from ~ 9000 to ~ 50 nm (Fig. 1(b) ① ② ③). The performance of induced nESI with a set of different tip diameters is consistent with that mechanism.

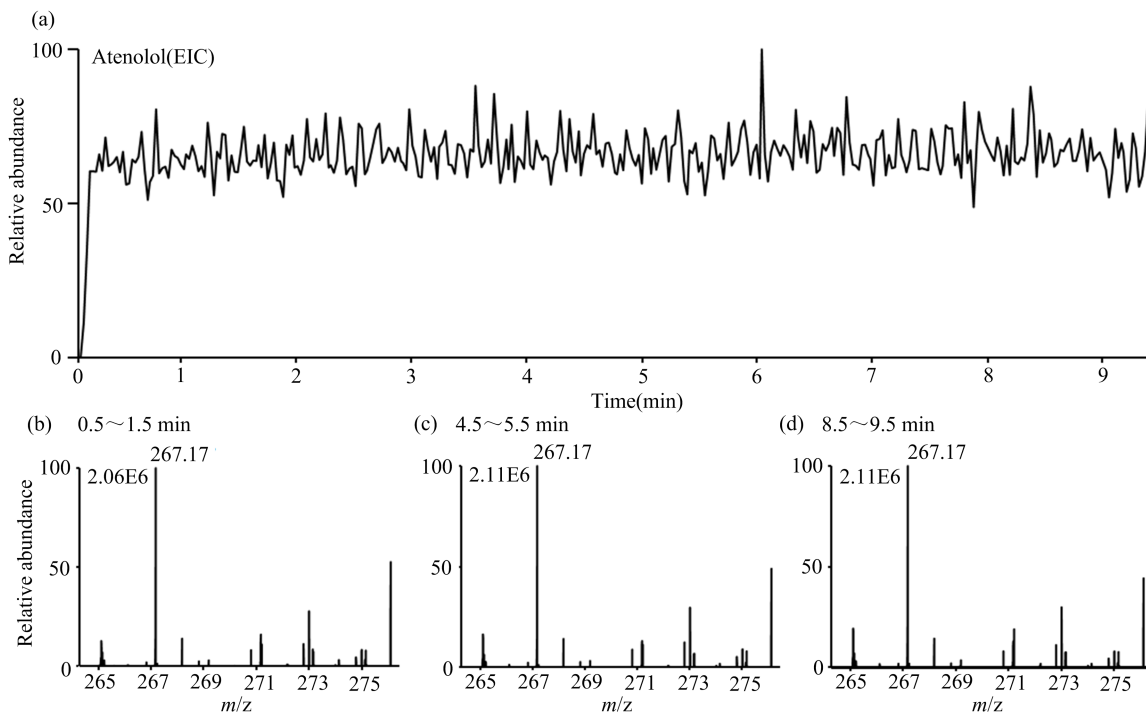


Fig. 4 (a) Extracted ion chromatogram and (b, c and d) mass spectra of atenolol (1ppm, $m/z = 267.17$) by induced nESI at different time intervals.

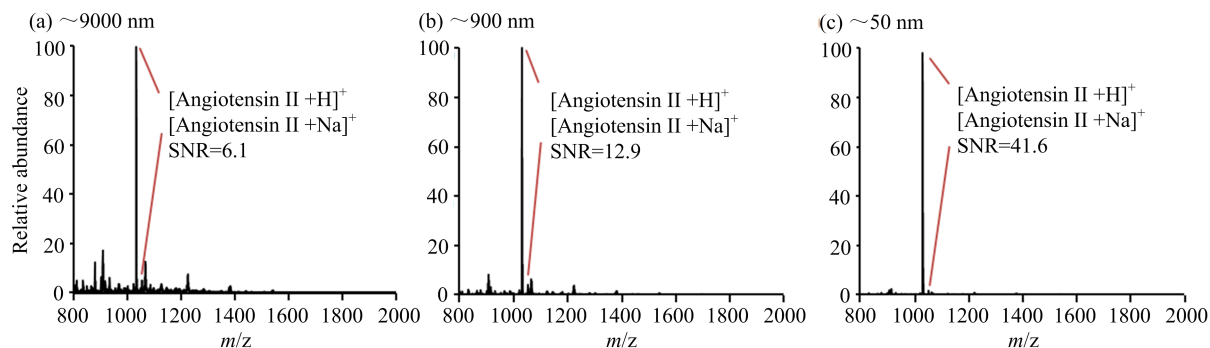


Fig. 5 The SNR of 10 ppm angiotensin II Tris buffer solution ($[M+H]^+$, $m/z=1032.8$; $[M+Na]^+$, $m/z=1054.7$) by induced nESI for a set of different tip diameters: (a) 6.1 for ~ 9000 nm, (b) 12.9 for ~ 1000 nm, (c) 41.6 for ~ 50 nm. (SNR = peak intensity of the molecule of interest/the strongest peak intensity of the matrices). The corresponding SEM images are shown in Fig. 1(b)①②③.

As clogging is mainly caused by nonvolatile inorganic salts, the influence of various inorganic salts on the spray time was investigated, and it was found that the spray time increases with solubility (Tab. 1). That is because the lower the solubility, the easier the salt precipitation. For induced nESI, we attempted to explore the influence of the alternating current frequency on spray time, and found that the ion current was stable for more than 5 min in a range from 500 to 5000 Hz (Fig. 6). Therefore, we selected 500 Hz as the optimum condition for the entire experiment.

Tab. 1 Comparison of spray time ($n=3$) among the three types of nonvolatile salts with different solubilities.

	Na_2HPO_4	NaCl	NaH_2PO_4
Salt concentration ($\text{mmol} \cdot \text{L}^{-1}$)	300	300	1200
Solubility ($\text{g} \cdot \text{L}^{-1}$)	77	360	869
Spray time (min)	0.12	8.77	>30.00

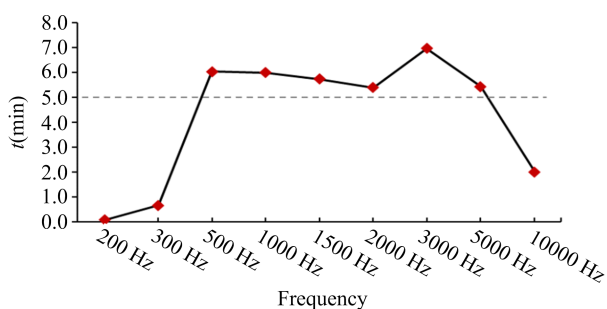


Fig. 6 Alternating current frequency optimization of spray time in induced nESI (time exceeding 5 min have been broken off intentionally).

To obtain relatively accurate flow rates of solvents with the same salt concentration in the capillary between the two ionization modes (Fig. 7), we chose a lower concentration of salt solution ($100 \text{ mmol} \cdot \text{L}^{-1}$ NaCl) that is passable for both modes, and obtained that the flow rate of conventional nESI ($35.7 \text{ nL} \cdot \text{min}^{-1}$) is slightly higher than that of induced nESI ($15.1 \text{ nL} \cdot \text{min}^{-1}$) (Tab. 2). As

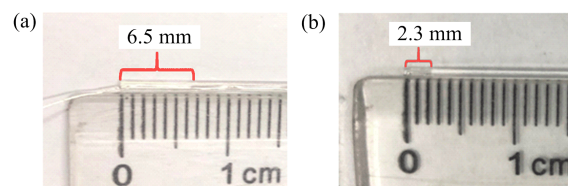


Fig. 7 Photographs of the distance from the end of the capillary that was totally filled with $100 \text{ mmol} \cdot \text{L}^{-1}$ NaCl solution to the position where the sample fluid level reached after 30 min of spraying, which was measure with a gauge. (a) 6.5 mm in conventional nESI. (b) 2.3 mm in induced nESI.

mentioned earlier, a solvent flow rate less than liquid evaporation rate near the tip would easily lead to salt deposition. Thus, we can infer that the lower flow rate of induced nESI is responsible for the mitigation of clogging. Although the droplet sizes were not confirmed by the measurements of flow rate, a lower flow rate results in a higher ionization efficiency^[24], which indicates that smaller initial droplet size is accompanied by lower flow rate. Finally, to illustrate whether the mitigation of capillary clogging is related to the alternative change of voltage polarity, the alternating current nESI, an ionization mode in which a silver electrode is inserted into a capillary with sample solution, was proved to have a similar effect to induced nESI, indicating that alternating voltage may help mitigate clogging (Fig. 8).

Tab. 2 Comparison of flow rates between conventional nESI and induced nESI for $100 \text{ mmol} \cdot \text{L}^{-1}$ NaCl ($n=3$).

	$t(\text{min})$	i.d.(min)	$\Delta d(\text{mm})$	Flow rate ($\text{nL} \cdot \text{min}^{-1}$)
Conventional nESI	30	0.5	6.5	35.7
Induced nESI	30	0.5	2.3	15.1

i.d. is the inner diameter of the capillary, and Δd is the distance from the end of the capillary that was totally filled with samples to the level of the sample fluid after spraying for 30 min. The flow rate can be calculated using the formula: $\text{Flow rate} = \frac{i.d.^2 \cdot \pi \cdot \Delta d}{4 \cdot t} \cdot 1000 \text{ nL} \cdot \text{min}^{-1}$. It is noted that the volume in the capillary (in 6.5 mm section) occupied by silver wire (o.d.=0.2 mm) should be subtracted in conventional nESI.

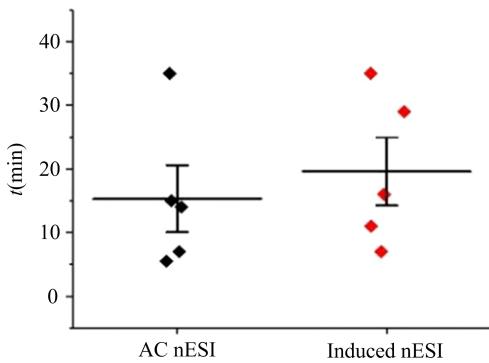


Fig. 8 Spray time distributions of the nanoemitters sprayed by representative alternating current (AC) nESI (black, $n = 5$) and induced nESI (red, $n = 5$) for mimic intracellular fluid.

3.4 Versatility of Induced alternating voltage on mitigating the clogging of mimic intracellular fluid and extracellular fluid

To demonstrate the versatility of induced nESI for mitigating clogging at the tip used directly in biochemical laboratories, mimic intracellular fluid (ICF) and extracellular fluid (ECF), which are high-salt buffers, were loaded into nanoemitters and then sprayed via induced nESI and conventional nESI, respectively. These artificial samples were prepared according to the literature^[25]. The protonated ions of atenolol [$C_{14}H_{22}N_2O_3 + H$]⁺ were formed from the two simulated samples using induced nESI and conventional nESI. The salt contents of the sample solutions are shown in Tab. 3.

As shown in Fig. 9(a), for mimic ECF, it is obvious that the nanoemitters could spray continuously and keep the ion current stable in induced nESI. The ion current

duration could reach more than 20 min. The capillary numbers with spray time of over 5 min accounted for 80% (8 out of 10 of the total capillaries). To save time we have artificially terminated the spray when the spray time was sustained for over 20 min. While using conventional nESI, the ratio was only 30%. Similar results were obtained for mimic ICF, as shown in Fig. 9 (b). When using induced nESI, the proportion of the capillary numbers with spray time exceeding 5 min was 90%. While in conventional nESI, the ratio was only 30%. Fig. 9(c),(d) are linear fitting graphs of the ionic strength to the concentration of the analyte. The calibration curves of atenolol concentration with three repeated measurements to illustrate the present method for mimic ECF and ICF were found to be linear with MS intensities in the ranges we tested (50-1500 ppb in ECF and 10-1000 ppb in ICF). Both above-mentioned calibrations, without external standards, were obtained with artificial cellular solution. Notably, the longest lifetime of tips can be up to two orders of magnitude more than the shortest. Therefore, it can be inferred that the utilization of induced alternating voltage in electrospray process can lengthen the spray time of capillaries effectively in most cases, thereby facilitating accurate quantitative analysis.

Tab. 3 Common chemical composition of mimic ECF and ICF (in $mmol \cdot L^{-1}$).

	NaCl	KCl	CaCl ₂	MgCl ₂	NaHCO ₃	Glucose	HEPES
ECF	143	5.3	1.8	2.1		10	10
ICF		140		29	10	10	10

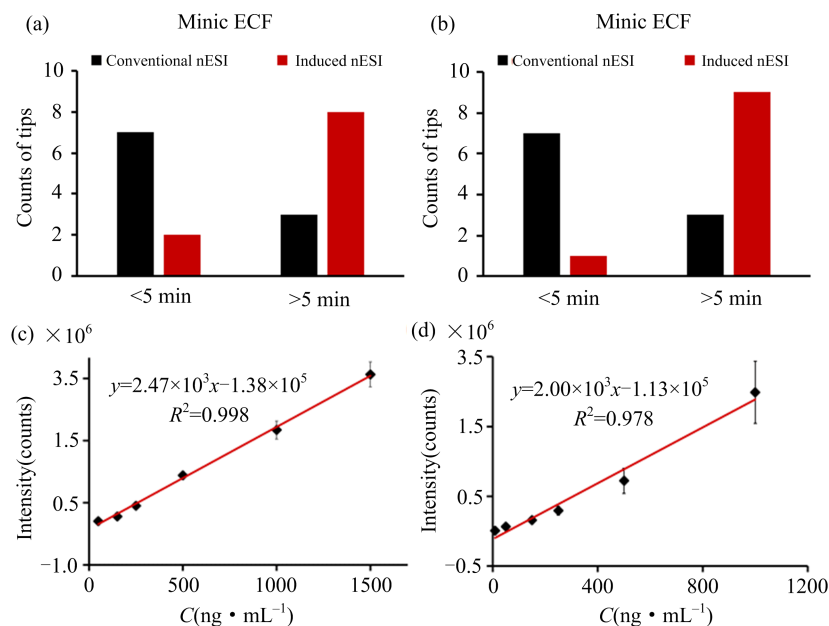


Fig. 9 Summary of the lasting time for the nanoemitters sprayed by conventional nESI ($n = 10$) and induced nESI ($n = 10$) for (a) mimic ECF and (b) mimic ICF. Calibration curve of atenolol concentration ($C(\text{ng} \cdot \text{mL}^{-1})$) in (c) mimic ECF and (d) mimic ICF.

4 Conclusions

In summary, induced alternating voltage was illustrated to enable the mitigation of capillary clogging during the submicro-nano electrospray ionization process. The possible mechanism for droplet formation on the outer surface of the nanoemitter, which will re-dissolve the crystallized salts derived from biological solutions, was explored. Additionally, the high performance of induced nESI under various conditions was investigated. Mimic ICF and ECF were both evaluated using induced nESI and conventional nESI, and the mitigating effect of the induced alternating voltage was also confirmed. The present study indicates that the induced alternating voltage can potentially serve as a widely feasible approach to adapting nESI with extremely small emitters to nonvolatile buffer systems.

Acknowledgements

This work was supported by the National Natural Science Foundation of China (21775143, 21475121), the Innovative Program of Development Foundation of Hefei Center for Physical Science and Technology (2017FXCX003), Users with Excellence Project of Hefei Science Center CAS (2018HSC-UE001, 2018HSC-UE016), and the Fundamental Research Funds for the Central Universities.

Conflict of interest

The authors declare no conflict of interest.

Author information

REN Mengting is currently pursuing her Master degree under the supervision of Prof. Huang Guangming Huang at University of Science and Technology of China. Her current research mainly focuses on induced nESI mass spectrometry.

HUANG Guangming (corresponding author) is currently a professor at University of Science and Technology of China. His research interests cover the basic theory of electrospray mass spectrometry, high-throughput mass spectrometry, and single cell mass spectrometry.

References

- [1] Wilm M, Mann M. Analytical properties of the nano electrospray ion source. *Anal. Chem.*, 1996, 68 (1): 1-8.
- [2] Karas M, Bahr U, Dülcks T. Nano-electrospray ionization mass spectrometry: addressing analytical problems beyond routine. *Fresenius' J. Anal. Chem.*, 2000, 366 (6): 669-676.
- [3] Susa A C, Xia Z, Williams E R. Native mass spectrometry from common buffers with salts that mimic the extracellular environment. *Angew. Chem. Int. Ed.*, 2017, 56 (27): 7912-7915.
- [4] Susa A C, Xia Z, Williams E R. Small emitter tips for native mass spectrometry of proteins and protein complexes from nonvolatile buffers that mimic the intracellular environment. *Anal. Chem.*, 2017, 89 (5): 3116-3122.
- [5] Hu J, Guan Q Y, Wang J, et al. Effect of nanoemitters on suppressing the formation of metal adduct ions in electrospray ionization mass spectrometry. *Anal. Chem.*, 2017, 89 (3): 1838-1845.
- [6] Wahl J H, Goodlett D R, Udseth H R, et al. Attomole level capillary electrophoresis-mass spectrometric protein analysis using 5-mm i.d. capillaries. *Anal. Chem.*, 1992, 64 (24): 3194-3196.
- [7] Wahl J H, Goodlett D R, Udseth H R, et al. Use of small-diameter capillaries for increasing peptide and protein detection sensitivity in capillary electrophoresis - mass spectrometry. *Electrophoresis*, 1993, 14 (1): 448-457.
- [8] Emmett M R, Caprioli R M. Micro-electrospray mass spectrometry: ultra-high-sensitivity analysis of peptides and proteins. *J. Am. Soc. Mass Spectrom.*, 1994, 5 (7): 605-613.
- [9] Koerner T, Turck K, Brown L, et al. Porous polymer monolith assisted electrospray. *Anal. Chem.*, 2004, 76 (21): 6456-6460.
- [10] Lee S S, Douma M, Koerner T, et al. An evaluation of the performance of porous polymer monolith assisted electrospray. *Rapid Commun. Mass Spectrom.*, 2005, 19 (18): 2671-2680.
- [11] Koerner T, Xie R, Sheng F, et al. Microsphere entrapped emitters for sample preconcentration and electrospray ionization mass spectrometry. *Anal. Chem.*, 2007, 79 (9): 3312-3319.
- [12] Rahman M M, Hiraoka K, Chen L C. Realizing nano electrospray ionization using disposable pipette tips under super atmospheric pressure. *Analyst*, 2014, 139 (3): 610-617.
- [13] Kelly R T, Page J, S, Luo Q, et al. Chemically etched open tubular and monolithic emitters for nano electrospray ionization mass spectrometry. *Anal. Chem.*, 2006, 78 (22): 7796-7801.
- [14] Huang G, Li G, Ducan J, et al. Synchronized inductive desorption electrospray ionization mass spectrometry. *Angew. Chem. Int. Ed.*, 2011, 50 (11): 2503-2506.
- [15] Huang G, Li G, Cooks R G. Induced nano electrospray ionization for matrix-tolerant and high-throughput mass spectrometry. *Angew. Chem. Int. Ed.*, 2011, 50 (42): 9907-9910.
- [16] Zhu H, Zou G, Wang N, et al. Single-neuron identification of chemical constituents, physiological changes, and metabolism using mass spectrometry. *Proc. Natl. Acad. Sci. U. S. A.*, 2017, 114(10):2586-2591.
- [17] Kulyk D S, Swiner D J, Sahraeian T, et al. Direct mass spectrometry analysis of complex mixtures by nano electrospray with simultaneous atmospheric pressure chemical ionization and electrophoretic separation capabilities. *Anal. Chem.*, 2019, 91(18): 11562-11568.
- [18] Flender C, Wolf C, Leonhard P, et al. Nano-liquid chromatography-direct electron ionization mass spectrometry: improving performance by a new ion source adapter. *J. Mass Spectrom.*, 2011, 46 (10): 1004-1010.
- [19] Pal S, Kulkarni A A. Interfacial precipitation and clogging in straight capillaries. *Chem. Eng. Sci.*, 2016, 153: 344-353.
- [20] Berkel G J V, Asano K G, Schmier P D. Electrochemical processes in a wire-in-a-capillary bulk-loaded, nano-electrospray emitter. *J. Am. Soc. Mass Spectrom.*, 2001, 12(7): 853-862.
- [21] Yeo L Y, Lastochkin D, Wang S C, et al. A new ac electrospray mechanism by Maxwell-Wagner polarization and capillary resonance. *Phys. Rev. Lett.*, 2004, 92 (13): 133902.
- [22] Gong X, Xiong X, Zhao Y, et al. Boosting the signal intensity of nano electrospray ionization by using a polarity-reversing high-voltage strategy. *Anal. Chem.*, 2017, 89(13):7009-7016.
- [23] Rahman M M, Ching K. Stable and reproducible nano-

- electrospray ionization of aqueous solutions and untreated biological samples using ion current limitation combined with polarity reversing. *Anal. Methods*, 2019, 11(2): 205-212.
- [24] Berggren W T, Westphall M S, Smith L M. Single-pulse nanoelectrospray ionization. *Anal. Chem.*, 2002, 74 (14): 3443-3448.
- [25] Tas A C. The use of physiological solutions or media in calcium phosphate synthesis and processing. *ActaBiomater.*, 2014, 10 (5): 1771-1792.

感应交流电延缓 nESI 中模拟生物样品引发的毛细管堵塞

任梦婷, 黄光明*

中国科学技术大学化学与材料科学学院化学系, 安徽合肥 230026

摘要: 生物样品的检测需要纳升电喷雾离子化质谱(nESI-MS)来适应更苛刻的条件,如高浓度的非挥发性缓冲液和亚微米尺寸的毛细管孔径.以上两个需求会给 nESI-MS 带来一个棘手的问题:毛细管堵塞.因此,为了延缓毛细管堵塞,我们将感应交流电压施加在尖端内径小于 $1\ \mu\text{m}$ 且注入高浓度盐溶液的毛细管上进行电喷雾.结果表明,改进后的毛细管比常规 nESI 下的毛细管寿命长 1~2 个数量级.较长的喷雾时间是由于电场方向周期性变化使析出的盐结晶再溶解从而延缓毛细管堵塞.同时,经过长时间(约 10 min)高浓度盐溶液的电喷雾,改进后的 nESI 仍保持稳定和灵敏的信号.最后对模拟细胞外液和细胞内液进行了验证,结果表明感应 nESI 是一种延缓毛细管堵塞的广泛适用的生物样品分析方法.

关键词: 感应 nESI; 生物样品; 堵塞; 亚微米级毛细管; 喷雾时间